Physica A: Statistical Mechanics and its Applications

Detecting Non-Uniform Structures in Oil-in-Water Bubbly Flow Experiments

--Manuscript Draft--

Manuscript Number:	PHYSA-233305R1
Article Type:	Research Paper
Section/Category:	Concepts or methods of statistical mechanics in Complex Systems and Complex Networks
Keywords:	Keywords: Bubbly flow; Non-uniform Bubble; Coalescence; VAE-GAN
Corresponding Author:	Meng Du, Ph.D. Tianjin University of Science and Technology TianJin, CHINA
First Author:	Meng Du, Ph.D.
Order of Authors:	Meng Du, Ph.D.
	Feifan Ren
	Rui Min
	Zhenqian Zhang
	Zhongke Gao
	Celso Grebogi
Abstract:	In this work, we first design a series of oil bubbly flow experiments in a vertical testing pipe, and collected the fluid fluctuations as experimental observations. Then we establish a Variational Autoencoder-Generative Adversarial Network (VAE-GAN) [1] from 4272 fluid time-frequency features, which is used to detect anomalous fluctuations in the experimental oil bubbly flow signals. These anomalous fluctuations are then utilized to experimentally identify the non-uniform flow structures in oil-in-water bubbly flow. In addition, by analyzing the identified non-uniform flow structures in a vertical 20mm inner diameter pipe, we investigate the oil bubbles coalescence phenomenon under various flow conditions. The impacts of mixed fluid velocity and phase volume fraction on the bubble coalescence behaviors are also investigated. The proposed method not only serves as an efficient tool for flow anomaly detection, but also provides a novel way to characterize the evolutionary behaviors of diverse bubbly flow systems.

Detecting Non-Uniform Structures in Oil-in-Water Bubbly Flow Experiments

Meng Du[a,*], Fei-fan Ren[a], Rui Min[b], Zhen-qian Zhang[a], Zhong-ke Gao[c] and Celso Grebogi[d]

[a]School of Electrical Engineering and Automation, Tianjin University of science and technology, Tianjin 300222, China

[b]Shandong Guangyu Technology Co., Ltd, Dongying Shandong 257000, China

[c]School of Electrical Engineering and Automation, Tianjin University, Tianjin 300072, China

[d]The Institute for Complex Systems and Mathematical Biology, King's College, University of Aberdeen, Aberdeen AB24 3UE, UK

ABSTRACT

In this work, we first design a series of oil bubbly flow experiments in a vertical testing pipe, and collected the fluid fluctuations as experimental observations. Then we establish a Variational Autoencoder-Generative Adversarial Network (VAE-GAN) [1] from 4272 fluid time-frequency features, which is used to detect anomalous fluctuations in the experimental oil bubbly flow signals. These anomalous fluctuations are then utilized to experimentally identify the non-uniform flow structures in oil-in-water bubbly flow. In addition, by analyzing the identified non-uniform flow structures in a vertical 20mm inner diameter pipe, we investigate the oil bubbles coalescence phenomenon under various flow conditions. The impacts of mixed fluid velocity and phase volume fraction on the bubble coalescence behaviors are also investigated. The proposed method not only serves as an efficient tool for flow anomaly detection, but also provides a novel way to characterize the evolutionary behaviors of diverse bubbly flow systems.

Keywords: Bubbly flow; Non-uniform Bubble; Coalescence; VAE-GAN;

1. Introduction

The oil-in-water bubbly flows are present in various fields such as petroleum, chemistry, biology, and others. The detection of occasional flow anomalies in oil bubbly flow, such as the non-uniform flow structures, is still an unsolved problem. And, understanding the dynamics of this kind of flow anomaly is of great importance in numerous multi-phase flow applications, such as pipeline pressure drop prediction and instrument design. Experimental tools, such as probe arrays [2], X-ray [3], microwave tomography [4], ultrasonic method [5], high frequency sensor [6], and PIV [7] have been employed to investigate behaviors of the oil bubbly flow. At the same time, the flow behaviors of oil bubbly flow are demonstrated with the experimental collected fluid conductance or pressure fluctuation signals. Time series analysis methods, including the joint time-frequency representation [8], wavelet analysis [9], recurrence plot [10], and complex network are [11] employed to reveal the bubbly flow evolutional dynamics [12], multi-scale features [13], and nonlinear characteristics [14].

Typically, the radial distribution of bubble flow is not homogeneous, neither the velocity nor the fraction profiles. Because of the oil bubble collision [15], some irregular non-uniform oil bubbles or bubble clusters are occasionally generated. This phenomenon, known as coalescence, is also observed and investigated in other multi-phase flow systems [16] [17]. In fact, the inhomogeneous velocity profile is thought to be one of the reasons for the formation of non-uniform bubbles, since the velocity gradient increases the bubble collision and the coalescence frequency. These non-uniform structures vary in shape, size, and evolutional dynamics, so that there are few objective criteria for identifying the non-uniform flow structures in oil-in-water bubbly flow. Especially, when these non-uniform flow bubbles are occasionally generated, it is difficult to model such a kind of flow anomaly, since most existing two-phase flow analysis models treat the oil bubbly flow as a stationary stochastic process. Therefore, developing a reliable and objective method to detect the non-uniform bubbles in oil-in-water bubbly flow, and further to model its evolutional dynamics becomes rather crucial and necessary.

Recently, machine leaning techniques have already been used as an effective tool for modelling various types of multi-phase flow data, such as flow snapshots [18], conductance fluctuations [19], flow rate [20] pressure [21], and temperature [22]. It has also been used in a variety of multi-phase flow applications, including the hold-up prediction [23], flow rate measurement [24], flow regime prediction [25], and flow pattern identification [26]. In particular, the state-of-the-art deep learning theory, which has made great progress in various fields [27] [28] [29], provides a novel way to perform data-based modelling of multi-phase flow system. The most common application of deep learning models for multiphase flows is flow pattern recognition. Du et al. [30] investigate the flow pattern recognition accuracy of the Convolutional Neural Network (CNN). They show that the CNNs with much deeper structures are more efficient in identifying the flow patterns. Cerqueira et al. [31] propose a deep CNN-based algorithm to identify and reconstruct the bubble shapes in bubbly flow images under the situation of high bubble overlapping. Poletaev et al. [32] use neural networks to recognize the bubble patterns in a turbulent bubbly jet. The deep learning methods have also been reported for predicting and measuring multi-phase flow parameters. Dang et al. [33] propose a flow parameter prediction model with deep CNN-LSTM network; the proposed model is utilized to measure the water-cut and mixture velocity of vertical oil-in-water two-phase flow. Zhao et al. [34] employ a deep neural network with eight layers to establish the mapping between the permittivity and water content of oil-water two-phase flow. Lin et al. [35] train a deep neural network with the phase velocity and pipe inclination angles, which is used to predict the flow regimes of the gas-liquid two-phase flow. Wang et al. [36] estimate the phase velocities of oil-gas-water three-phase flow with three models, which are deep neural network (DNN), convolutional neural

network (CNN), and support vector machine (SVM). They find that DNN and SVM models are more suitable for the multi-phase flow rate prediction. Other applications of deep learning methods to the multi-phase flow system involve bubble location [37], flow image super resolution [38], flow tomography [39], computational fluid dynamics (CFD) models [40], and micro-fluid dynamics [41]. The advantages of using machine learning methods to solve multi-phase flow problems are manifold. It ignores the complex multi-phase flow dynamics, which is quite difficult to model theoretically, and the established data-driven model-free method is regarded as an alternative tool for characterizing the multi-phase flow behaviors.

However, most of these applications focus mainly on the long-range statistical characteristics of the two-phase flow system, and a large quantity of prior labeled data is needed for establishing the machine learning (deep learning) model. Note that, the oil bubbly flow systems typically exhibit long-range stable and stochastic characteristics, making it difficult for most data-driven methods to capture the sparsely unpredictable anomalies, such as the generation of non-uniform bubble clusters. The novelty and goal of this research is to develop an efficient tool that can identify the non-uniform flow structures in vertical oil bubbly flow using a smaller training data set. In this paper, we employ the generating adversarial framework and establish a VAE-GAN based deep learning model, which can serve as a novel tool for detecting non-uniform flow structures from the stochastic bubble flow. Furthermore, we experimentally investigate the oil bubble coalescence dynamics by analyzing the flow behaviors of the detected non-uniform flow structures.

The remainder of this paper is organized as follows. In the next section, we describe our oil-in-water bubbly flow experiment in a vertical 20mm inner diameter pipe. The collected oil bubbly fluctuation signals are also presented. In Section 3, we present a Variational Autoencoder-Generative Adversarial Network (VAE-GAN) based machine framework, which is applied to identify the non-uniform flow structures in the oil bubbly flow experimental system. Section 4 presents the homogeneous flow structure identification results. Also, the oil bubble coalescence behaviors are analyzed in this Section. The conclusions are in Section 5.

2. The Oil-in-Water Bubbly Flow Experiment

We carry out a flow loop experiment to collect the fluid fluctuation signals, which are used as observations to investigate the dynamical flow behaviors of discrete oil bubbles. As shown in Fig. 1, the flow loop consists of a water tank, an oil tank, a mixing tank, two metering pumps, and a section of a 20mm inner diameter vertical plastic testing pipe. In the experiment, we use the pre-calibrated metering pumps to control the phase velocity of oil and water. The experiment schedule is as follows: we first adjust the flow rate of the two phases to reach a preset volume fraction and mixture velocity. Once the oil and water are well mixed, the fluid conductance fluctuation signals are collected. This measuring procedure is repeated under various flow conditions, with the mixture velocity set at 0.073m/s, 0.11m/s, 0.147m/s, 0.184m/s, 0.221m/s, and 0.258m/s. The water phase volume fraction is varied in the range of 70-100%, with a step of 2% increment.

We employ the four-ring conductance sensor [42], which was first designed to measure the water-cut of the two-phase flow under high water phase volume fraction conditions. As shown in Fig. 1, the conductance sensor consists of four stainless steel conductance rings, which are axially separated and fixed on the inside wall of the testing pipe. E_1 and E_2 are the excitation electrodes that are connected to a 100 kHz sinusoidal signal. M_1 and M_2 are the measuring electrodes that the conductance fluctuating signals measured from M_1 and M_2 are mainly correlated with the fluid fluctuations and dynamics. The fluid conductance fluctuations measured from the conductance sensor are commonly used as experimental observations to quantitively characterize the multi-phase flow behaviors. In this study, the training and testing data set of the proposed VAE-GAN based machine learning framework both come from the experimental measured fluid fluctuations. Anomaly fluctuation segments are identified by the well-trained VAE-GAN network, and further analyzed to characterize the oil bubble coalescence behaviors.

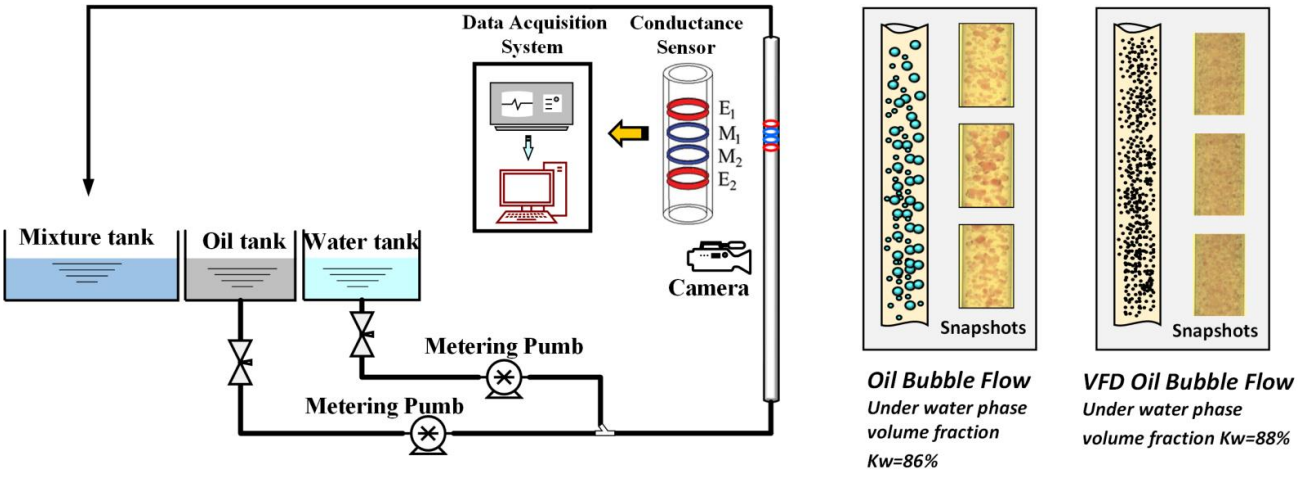

Fig. 1: The schematic of the oil-in-water bubbly flow loop.

In the experiment, we have observed two types of typical oil-in-water bubbly flow patterns [43], they are the discrete Oil Bubble Flow and Very Fine Dispersed (VFD) Oil Bubble Flow. As shown in figure 1, i) Oil bubble flow: observed under lower mixture flow rate, discrete and visible oil bubbles uniformly distributed in the continuous water phase; ii) VFD Oil bubble flow: observed at higher mixture flow rate, the oil bubbles are broken into invisible small droplets, which are also uniformly distributed in water.

The flow behaviors of the oil-in-water bubbly flow are characterized with the collected fluid conductance fluctuation signals. In most situations, these fluctuation signals are noise like, which reveals the stochastic flow behavior of the dispersed oil phase. However, in our experiment, we occasionally observe anomalous fluctuations in the collected signals that do not appear to be part of the stochastic background. These anomalous fluctuations are thought to be related to the non-uniform flow structures in the oil bubbly flow, as the presence of large bubbles or bubble clusters cause a sudden change in the conductivity of the fluid mixture. Figure 2 shows some of the fluid fluctuation signal segments containing anomalous fluctuations. We find that the background of these fluctuation signals is noisy like, indicating the stochastic flow behaviors of the oil bubbles/droplets. However, the amplitude and frequency of the anomalous fluctuations are different from the background signals due to the coalesced oil bubble clusters.

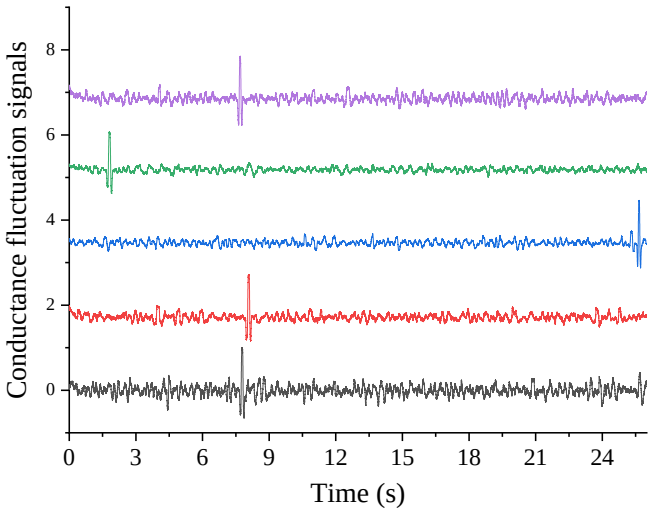

Fig.2: The experimental oil bubbly flow fluctuation signals containing anomaly fluctuations.

Traditional fluid fluctuation analysis methods are inefficient for identifying the non-uniform structures in oil-in-water bubbly flow. Because the uniform bubbles and bubble clusters vary with size and morphology, and there are no objective criteria for distinguishing the anomalous fluctuation from the stochastic background. In this regard, we turn to a semi-supervised data-driven framework, which we introduce in the next section, to investigate the dynamical behaviors of non-uniform flow structures in oil bubble flow.

3. VAE-GAN based framework for identifying the non-uniform flow structures

The oil bubble coalescence [15], which is attributed to the collisions, is thought to be the main reason for the generation of the non-uniform flow structures in bubbly flow system. Normally, the bubble flow can be considered as a stationary stochastic process in which the fluid fluctuations are noisy-like random signals. However, the fluctuations, which correspond to the non-uniform flow structures, are distinguished from the noisy signal background. In this respect, we can treat these non-uniform fluctuations as anomalies, and locate these anomalies in the noisy like fluid fluctuation signals as an effective way to detect the non-uniform structures in the oil bubble flow.

Inspired by this, we developed a machine learning model for the flow anomaly detection. We employ the structure of VAE-GAN and trained the model with empirically selected stochastic background signals. This allows the model to learn the noise features and describe the stochastic characteristics of the bubbles. When testing, we reconstruct the test signal segments with our designed model, and we deem it anomalous if the reconstruction error is higher than a predetermined threshold, indicating a significant deviation of the test signal from the stochastic background.

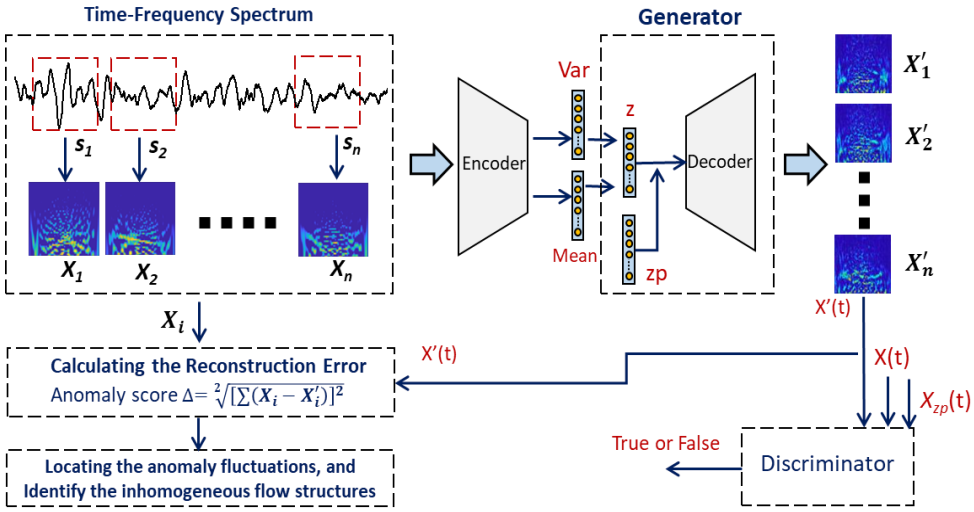

Fig. 3: The schematic of VAE-GAN based model for non-uniform flow structure identification.

Figure 3 shows the schematic of our established machine learning model, which is used for identifying the non-uniform flow structures in oil bubbly flow system. First, the experimental collected conductance signals are segmented with a window to obtain the training data set s_i. Then, we calculate the quadric time-frequency spectra X_i of each signal segment in s_i, which are employed as the input of a VAE-GAN. The calculated time-frequency spectra are encoded by the VAE-Encoder to generate a sampled latent representation Z, and reconstructed from the VAE-GAN's generator by combining the generated latent vector Z with a Gaussian distribution Z_p. The discriminator of VAE-GAN evaluates the reconstructed time-frequency spectrum and guarantees the resemblance of the generated time-frequency spectrum to the input data. When testing, we calculate the reconstruction error of the generated time-frequency representation and the input spectrum, which is defined as,

$$\Delta = \sqrt{(X_i - X_i')^2} \tag{1}$$

where X_i refers to the input time-frequency spectrum, and $X\,i$ is the reconstructed spectrum. If the reconstructed error Δ is larger than a preset threshold, we conclude that the input is distinguishable from most of the noisy like background. In this work, we choose the maximum reconstruction error ($\Delta' = max\,\Delta$) of the training data set as the threshold for identifying the actual anomalous fluctuation signals. In this way, the anomaly fluctuations, which indicate the existence of non-uniform flow structure in the oil bubbly flow, are identified. Additionally, it is noted that the proposed network is trained semi-supervised, and the training data are manually labeled, which limits the size of the training data set. We can address this issue by turning to an unsupervised framework, however, this involves extensive experiment data preparation. Another limitation of using the proposed method is the restriction to the experimental data, which requires that the anomaly be sparsely generated. Experimental observations that include frequent anomalies are not suitable for use as training data.

In this work, we use the Wigner-Ville representation method [44] [45] to calculate the joint quadric time-frequency spectrum of the training data. We employ the time-frequency spectrum as the VAE-GAN's input instead of the original fluid fluctuation signal for the following reasons. Firstly, the time-frequency spectrum is a powerful two-phase flow characterizing tool [46] [47], and the joint time-frequency representations are rich in fluid dynamic information, such as the complexity [48], the motion frequency of discrete bubbles [49], the flow pattern transition [50], and the fluctuation energy of the fluid [51]. This makes the time-frequency spectra to offer clear and efficient features of the flowing oil bubbles. Secondly, we use the quadratic time-frequency distribution, which involves a quadratic component in its computation. This enlarges the gap between the spectrum of anomalous fluctuations and the background noise, which makes it easier to identify non-uniform flow structures. Note that, as typical generative adversarial model, the VAE-GAN has demonstrated excellent performance and gained significant achievements in the field of anomaly detection [52][53][54]. The discriminator, which we employ a convolutional neural network architecture, identifies the generated time-frequency representation and improves the accuracy of the reconstructed time-frequency representations with iterative corrections.

When testing, in order to capture the features of the non-uniform flow structures in oil bubbly flow, the window, which is utilized to segment the testing fluctuation signals, needs to be long enough to enclose an entire anomalous fluctuation. In the experiment, we find that most anomalous fluctuations last no longer than 2 second. Therefore, we choose the length of the segmentation window to be last 2 second. We empirically select in total of 4272 training segments, which correspond to the fluctuation background from the collected fluctuation signals. Figure 4 shows typical signals segments, which are utilized for training the non-uniform flow structure detecting model.

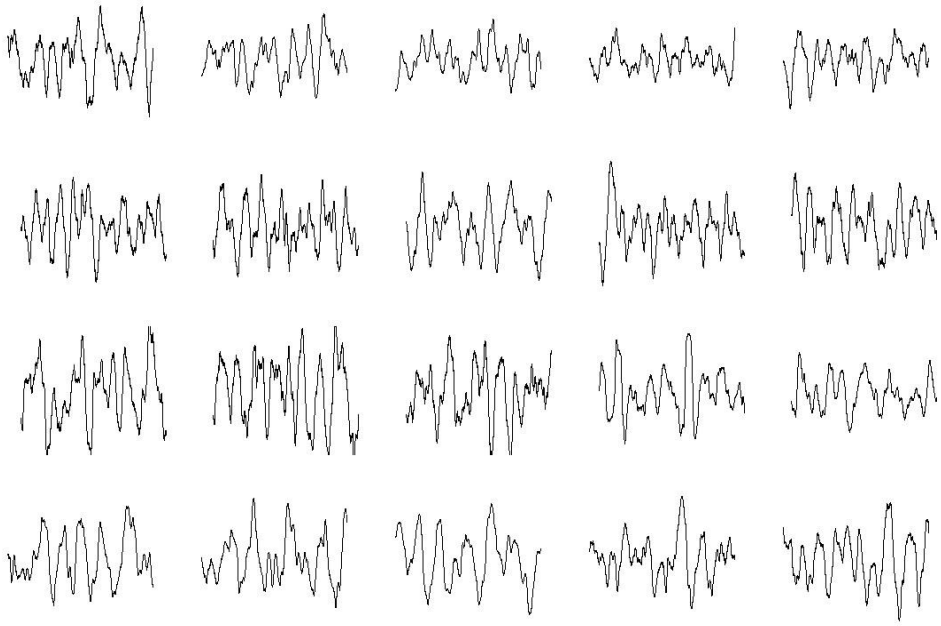

Fig. 4: The fluctuation signals used for training the VAE-GAN model (2 seconds)

Table 1 show the comparisons of the input and the reconstructed time-frequency spectra under uniform and non-uniform flow conditions, respectively. As shown in the first column, under the uniform flow condition, the input time-frequency spectra are lower in energy, indicating a stable flow behavior of the bubble flow. We also notice that the energy distributions in the spectrum are uniformly distributed, which characterize the stochastic flow behavior of the uniform bubbles. The reconstructed time-frequency spectra of uniform fluctuations are shown in the second column in Table 1. The stable and stochastic characteristics of the uniform flow are retained in the reconstructed time-frequency spectrum. The reconstructed time-frequency representations also have lower energy and show a uniform distribution.

As for the non-uniform flow, the input time-frequency spectra, which are shown in the third Colum of Table 1, display as higher energy and non-uniform energy distribution, indicating the unstable and non-uniform flow behaviors of the occasionally generated non-uniform bubbles and bubble clusters. However, as shown in the fourth column in Table 1, the reconstructed time-frequency spectra of non-uniform flow are uniform distributed with lower energy. This implies that the unstable flow behaviors of non-uniform bubble flow are not well reconstructed from the input time-frequency representations. In this respect, the reconstruction error Δ defined in Eq. (1) can serve as a criterion for identifying the non-uniform flow structures.

Table 1

The comparisons of the input and the reconstructed time-frequency spectra

Segments under uniform flow		Segments under non-uniform flow	
Input time-frequency spectrum	Reconstructed time-frequency spectrum	Input time-frequency spectrum	Reconstructed time-frequency spectrum
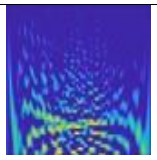	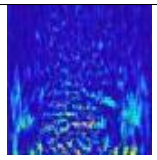	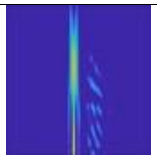	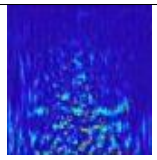
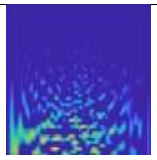	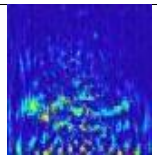	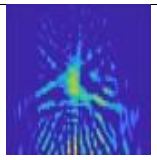	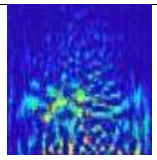
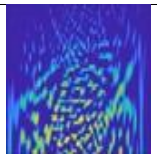	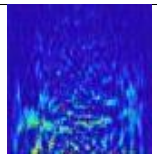	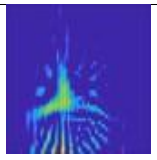	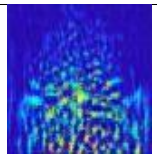
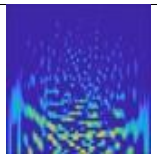	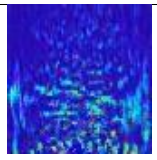	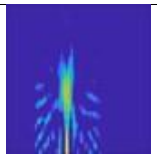	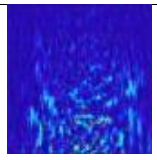

4. Non-uniform Flow behaviors and the Oil Bubble Coalescence Dynamics in Vertical Pipe

It is thought that the generation of non-uniform flow structures in the bubbly flow system is attributed to bubble coalescence. However, the mechanism of coalescence in a bubble flow system is very complex due to Wake effects [55], turbulence [56], buoyancy [57], and pipe wall friction [58], these being some of the reasons. To characterize the non-uniform flow behaviors of bubbly flow system and further investigate the bubble coalescence dynamics, we in this work analyze the correlation between the number of detected non-uniform flow structures and the flow conditions, such as flow rate, water-cut, and the flow patterns.

The non-uniform flow structures in our bubbly flow system are identified with the proposed VAE-GAN based framework, and we count the number of detected non-uniform flow structures from the testing fluctuation signals under different flow conditions. The duration of each testing signal is set as the same length, which is 30 seconds. Figure 5 shows the number of detected non-uniform flow structures under different mixed fluid velocities. In the low velocity region, where the mixture velocity $U\,m$ is in the range of $0.073m/s$ –$0.184m/s$, the number of generated non-uniform flow structures grows with increasing the mixed fluid velocity. However, under high mixed velocities (the mixture velocity $U\,m$ in the range of $0.221m/s$ –$0.258m/s$), the number of generated non-uniform flow structures in oil bubbly flow gradually decreases with increasing the mixed fluid velocity.

Note that there exists flow pattern transition from the low velocity region to the high velocity region, i.e., the flow patterns change from the oil bubble flow to the very fine dispersed oil bubble flow. One of the fluid dynamics that we have found in this study is that the oil bubble coalescence behaviors are not only related to the mixture velocity, but also related to the flow pattern. When the flow pattern changes from bubble to dispersed droplets (VFD oil bubble flow), as shown in Fig. 5, there exists obvious reversal of the dominant bubble interaction dynamics, i.e., from coalescence to break up. For the oil bubble flow pattern in our vertical oil-in-water flow system, when increasing the mixed fluid velocity, the intensity of fluid turbulence is enhanced, resulting in more frequent collisions and the consequent coalescence in the oil bubbly flow. In addition, the velocity gradient in the radial direction is enlarged with increasing mixed fluid velocity, which also increases the frequency of bubble coalescence in the radial direction. Therefore, in the low velocity region of Fig. 5, where the flow pattern is oil bubble flow, a larger number of non-uniform flow structures are generated with increasing the mixed fluid velocity. However, when the mixed fluid velocity reaches up a relatively high range (high velocity regime in Fig. 5, $U\,m$ = $0.221m/s$ – $0.258m/s$), the turbulence of the fluid is strong enough to break up the oil bubbles into smaller oil droplets, which is known as the very fine dispersed oil bubble flow. Under this flow pattern, the fluid turbulence intensity is high enough to break the oil phase into dispersed and uniform distributed oil droplets. Under this situation, the bubble breakup becomes the dominant phenomenon in the mixed fluid, and the breakup behavior gets more prevalent as the mixing velocity increases, resulting that the number of generated non-uniform flow structures begins to decrease gradually with increasing the mixed fluid velocity.

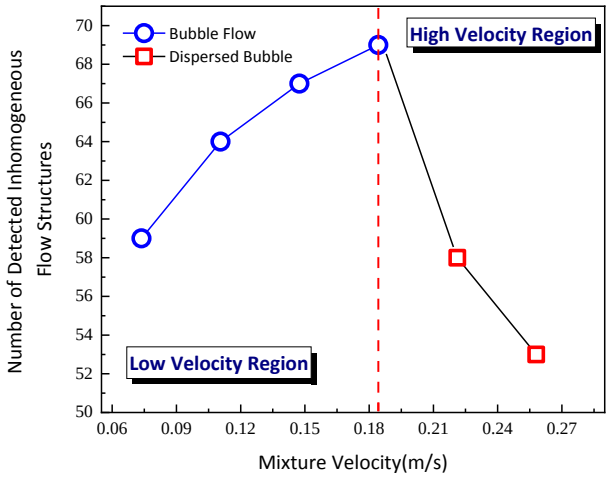

Fig. 5: The number of detected non-uniform flow structures in oil bubbly flow under different mixed fluid velocities.

We also investigate the coalescence behaviors of the oil-in-water bubbly flow under different phase volume fractions. We find that the bubble density is also a factor that impacts the coalescence behaviors in the vertical oil bubble flow system. As shown in Fig. 6, there exist more non-uniform flow structures in area I than that in high water phase volume fraction conditions (area II). In the experiment, under lower water phase volume fraction (area I), the oil bubbles show denser characteristics, which means more coalescence is happening under such flow conditions. With gradually increasing the water phase volume fraction, once a critical point (around 85%) is reached, the oil bubbles begin to show scattered distributions. The number of generated non-uniform flow structures gradually decreases with increasing the water phase volume fraction, indicating that the frequency of oil bubble collisions and coalescence are gradually reduced at higher water-ratio conditions.

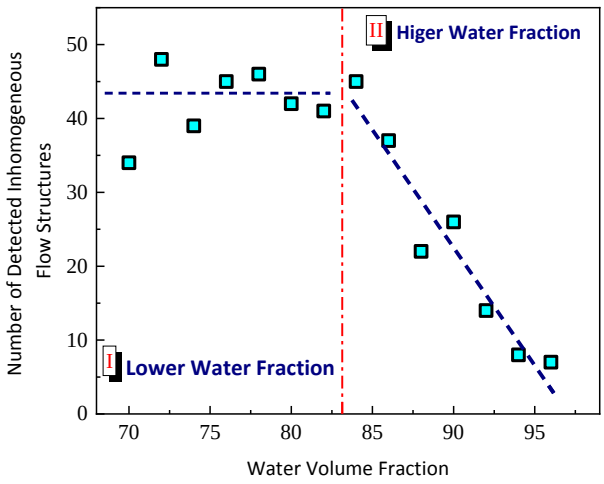

Fig. 6: The number of detected non-uniform flow structures in oil bubbly flow under different water phase volume fraction.

5. Conclusions

In this paper, we design a two-phase flow experiment in a vertical testing pipe to generate the desired oil-in-water bubble flow patterns: the oil bubble flow, and the very fine dispersed oil bubble flow. In the experiment, we also collect the oil bubble flow fluctuation signals with a conductance sensor. These experimental fluid fluctuation signals are then used as observations for analyzing the flow behaviors of oil bubbles. We propose a semi-supervised machine learning model for detecting the non-uniform structures in oil bubbly flow. We first calculate the quadric time-frequency spectra of the experimentally measured oil-in-water bubble flow fluctuation signals. Then the obtained time-frequency representations are fed in to a VAE-GAN as input, and the reconstruction error of the time-frequency representation are then used as criteria for identifying the non-uniform flow structures. Testing results of our experimental data set show that the proposed machine learning framework is efficient in detecting the non-uniform flow structures in the vertical oil bubbly flow system.

Furthermore, with the identified non-uniform flow structures, we investigate bubble flow behaviors and the oil bubble coalescence dynamics. We find that the coalescence behaviors in the vertical oil bubbly flow system depend on both the mixed fluid velocity and phase volume fraction. We also use the number of detected non-uniform flow structures to quantitatively indicate the bubble coalescence behaviors. Within the velocity range in our experiment (from 0.073m/s to 0.258m/s), the number of the generated non-uniform flow structures first increases from 59 to 69, and then gradually decreases to 53, which indicates the reversal of the dominant bubble interaction dynamics, i.e., from coalescence to break up. Also, we find that as the water phase volume fraction increases to around 85%, the number of generated non-uniform flow structures begins to decrease, indicating that bubble collisions and coalescence in an oil bubbly flow system are closely related to the density of the discrete phase.

The machine learning models are effective tools for interpreting the observations from physical systems and further discovering the underlying dynamics. The proposed semi-supervised network provides a novel way for analyzing the flow pattern evolutionary dynamics in multi-phase flow systems. Furthermore, this machine learning based method could have broader applications in other physical systems that are impacted by unknown anomalies. Unpredictable anomalies are identified with the well-trained network, and then the intrinsic mechanisms of the anomaly can be investigated.

6. Acknowledgements

This work was supported in part by the National Natural Science Foundation of China, under Grant 62373278, 52378254 and 41704131, and in part by the National Natural Science Foundation of Tianjin, China, under Grant 21JCJQJC00130, and in part by the Taishan Industrial Experts Program.

7. References

[1] A.B.L. Larsen, S.K. Sønderby, H. Larochelle, and O. Winther. Autoencoding beyond pixels using a learned similarity metric. In *International conference on machine learning*, pages 1558–1566, 2016.

[2] G.W. Govier, G.A. Sullivan, and R.K. Wood. The upward vertical flow of oil-water mixtures. Can. J. Chem. Eng., 39(2):67–75, 1961.

[3] B. Hu, M. Langsholt, L. Liu, P. Andersson, and C. Lawrence. Flow structure and phase distribution in stratified and slug flows measured by x-ray tomography. Int. J. Multiphase Flow, 67:162–179, 2014.

[4] M. Mallach, P. Gebhardt, and T. Musch. 2D microwave tomography system for imaging of multiphase flows in metal pipes. Flow Meas. Instrum., 53:80–88, 2017.

[5] F. Dong, H. Gao, W.L. Liu, and C. Tan. Horizontal oil-water two-phase dispersed flow velocity profile study by ultrasonic doppler method. Exp. Therm. Fluid. Sci., 102:357–367, 2019.

[6] J. Ma, N.D. Jin, D.Y. Wang, D.Y. Liu, and W.X. Liu. Measurement of water holdup in vertical upward high water-cut oil-in-water flows using a high frequency sensor. Sensor Actuat. A-Phys., 289:165–179, 2019.

[7] Y.C. Song, Y.Q. Shentu, Y.L. Qian, J.L. Yin, and D.Z. Wang. Experiment and modeling of liquid-phase flow in a venturi tube using stereoscopic PIV. Nucl. Eng. Technol., 53(1):79–92, 2021.

[8] H.M. Prasser, E. Krepper, and D. Lucas. Evolution of the two-phase flow in a vertical tube-decomposition of gas fraction profiles according to bubble size classes using wire-mesh sensors. Int. J. Therm. Sci., 41(1):17–28, 2002.

[9] X.S. Zhang, J.H. Wang, and D.C. Wan. An improved multi-scale two phase method for bubbly flows. Int. J. Multiphase Flow., 133:103460, 2020.

[10] H.W. Li, J.P. Liu, Y.L. Zhou, and B. Sun. Analysis of the nonlinear dynamic characteristics of two-phase flow based on an improved matrix pencil method. Chinese J. Chem. Eng., 24(6):737–748, 2016.

[11] B. Sun, E.P. Wang, Y. Ding, H.Z. Bai, and Y.M. Huang. Time-frequency signal processing for gas-liquid two phase flow through a horizontal venturi based on adaptive optimal-kernel theory. Chinese J. Chem. Eng., 19(2):243–252, 2011.

[12] T. Wei, X.C. Li, and D.X. Wang. Identification of gas-liquid two-phase flow patterns in dust scrubber based on wavelet energy entropy and recurrence analysis characteristics. Chem. Eng. Sci., 217:115504, 2020.

[13] R. Mosdorf and G. Górski. Detection of two-phase flow patterns using the recurrence network analysis of pressure drop fluctuations. Commun. Heat Mass., 64:14–20, 2015.

[14] Q.M. Sun and B. Zhang. Nonlinear characterization of gas liquid two-phase flow in complex networks. Exp. Therm. Fluid Sci., 60:165–172, 2015.

[15] Y. Liao and D. Lucas. A literature review on mechanisms and models for the coalescence process of fluid particles. Chem. Eng. Sci., 65(10):2851–2864, 2010.

[16] C.S. Daw, C.E.A. Finney, M. Vasudevan, N.A. Van Goor, K. Nguyen, D.C. Bruns, E.J. Kostelich, C. Grebogi, E. Ott, and J.A. Yorke. Selforganization and chaos in a fluidized bed. Phys. Rev. Lett., 75(12):2308, 1995.

[17] T. Nishikawa, Z. Toroczkai, and C. Grebogi. Advective coalescence in chaotic flows. Phys. Rev. Lett., 87(3):038301, 2001.

[18] G. Manfredo, B. Beatrice, S. Giorgio, and M.C.L. Pietro. Image-based analysis of intermittent three-phase flow. Int. J. Multiphase Flow., 107:256–262, 2018.

[19] H. Wang, S. Beck, G.H. Priestman, and R.F. Boucher. Fluidic pressure pulse transmitting flowmeter. Chem. Eng. Res. Des., 75(4):381–391, 1997.

[20] Y. Zhang, A.N. Azman, K.W. Xu, C. Kang, and H.B. Kim. Two-phase flow regime identification based on the liquid-phase velocity information and machine learning. Exp. Fluids., 61:212, 2020.

[21] A. Shahdi and M. Arabloo. Application of SVM algorithm for frictional pressure loss calculation of three phase flow in inclined annuli. Pet. Environ. Biotechnol., 5(3):1000179, 2014.

[22] W. Xu, Z. Fan, M. Cai, Y. Shi, X. Tong, and J. Sun. Soft sensing method of LS-SVM using temperature time series for gas flow measurements. Metrol. Meas. Syst., 22(3):383–392, 2015.

[23] C. Zhang, T. Zhang, and C. Yuan. Oil holdup prediction of oil–water two phase flow using thermal method based on multiwavelet transform and least squares support vector machine. Expert Syst. Appl., 38(3):1602–1610, 2011.

[24] M.A. Ahmadi, M. Ebadi, A. Shokrollahi, and S.M.J. Majidi. Evolving artificial neural network and imperialist competitive algorithm for prediction oil flow rate of the reservoir. Appl. Soft Comput., 13(2):1085–1098, 2013.

[25] J.E. Juliá, Y. Liu, S. Paranjape, and M. Ishii. Upward vertical two-phase flow local flow regime identification using neural network techniques. Nucl. Eng. Des, 238(1):156–169, 2008.

[26] L. Zhang and H. Wang. Identification of oil–gas two-phase flow pattern based on SVM and electrical capacitance tomography technique. Flow Meas. Instrum., 21(1):20–24, 2010.

[27] M. Frid-Adar, I. Diamant, M. Amitai E. Klang, J. Goldberger, and H. Greenspan. GAN-based synthetic medical image augmentation for increased CNN performance in liver lesion classification. Neurocomputing, 321:321–331, 2018.

[28] J. Zhao, X. Mao, and L. Chen. Speech emotion recognition using deep 1D & 2D CNN LSTM networks. Biomed. Signal Process. Control., 47:312–323, 2019.

[29] M. Simão, P. Neto, and O. Gibaru. EMG-based online classification of gestures with recurrent neural networks. Pattern Recogn. Lett., 128:45–51, 2019.

[30] M. Du, H.Y. Yin, X.Y. Chen, and X.Q. Wang. Oil-in-water two-phase flow pattern identification from experimental snapshots using convolutional neural network. IEEE Access, 7:6219–6225, 2018.

[31] R. Cerqueira and E.E. Paladino. Development of a deep learning-based image processing technique for bubble pattern recognition and shape reconstruction in dense bubbly flows. Chem. Eng. Sci., 230:116163, 2021.

[32] I. Poletaev, M.P. Tokarev, and K.S. Pervunin. Bubble patterns recognition using neural networks: Application to the analysis of a two-phase bubbly jet. Int. J. Multiphase Flow, 126:103194, 2020.

[33] W. Dang, Z. Gao, L. Hou, D. Lv, S. Qiu, and G. Chen. A novel deep learning framework for industrial multiphase flow characterization. IEEE T. Ind. Inform., 15(11):5954–5962, 2019.

[34] C. Zhao, G. Wu, and Y. Li. Measurement of water content of oil-water two-phase flows using dual-frequency microwave method in combination with deep neural network. Measurement, 131:92–99, 2019.

[35] Z. Lin, X. Liu, L. Lao, and H. Liu. Prediction of two-phase flow patterns in upward inclined pipes via deep learning. Energy, 210:118541, 2020.

[36] H. Wang, M. Zhang, and Y. Yang. Machine learning for multiphase flowrate estimation with time series sensing data. Measurement: Sensors, 10:100025, 2020.

[37] T. Haas, C. Schubert, M. Eickhoff, and H. Pfeifer. BubCNN: Bubble detection using faster RCNN and shape regression network. Chem. Eng. Sci., 216:115467, 2020.

[38] Z. Gao, Z. Qu, H. Wang, and C. Ma. Characterization of two-phase flow structure by deep learning-based super resolution. IEEE T Circuits-II, 68(2):782–786, 2020.

[39] Z. Xu, F. Wu, Y. Yang, and Y. Li. ECT attention reverse mapping algorithm: visualization of flow pattern heatmap based on convolutional neural network and its impact on ECT image reconstruction. Meas. Sci. Technol., 32(3):035403, 2020.

[40] H. Bao, J. Feng, N. Dinh, and H. Zhang. Computationally efficient CFD prediction of bubbly flow using physics-guided deep learning. Int. J. Multiphase Flow, 131:103378, 2020.

[41] C. Shen, Q. Zheng, M. Shang, and L. Zha. Using deep learning to recognize liquid-liquid flow patterns in microchannels. AIChE J., 66(8): e16260, 2020.

[42] M. Du, N. D. Jin, Z. K. Gao, Z. Y. Wang, and L. S. Zhai. Flow pattern and water holdup measurements of vertical upward oil-water two-phase flow in small diameter pipes, Int. J. Multiphase Flow 41: 91-105, 2012.

[43] L. S. Zhai H. X. Zhang Y. F. Han, N. D. Jin and Y. Y. Ren. Flow pattern and holdup phenomena of low velocity oil-water flows in a vertical upward small diameter pipe. J. Petrol. Sci. Eng., 159:387–408, 2017.

[44] E. Wigner. On the quantum correction for thermodynamic equilibrium. Phys. Rev., 40(5):749, 1932.

[45] J. Ville. Theorie et applications de la notion de signal analytique, cables et transmissions 2A, 61-74. Technical report, Rand corporation technical report, 1958.

[46] Z. He, D. Zhang, B. Cheng, and W. Zhang. Pressure-fluctuation analysis of a gas-solid fluidized bed using the wigner distribution. AIChE J., 43(2):345–356, 1997.

[47] M. Du, N.D. Jin, Z.K. Gao, Z.Y Wang, and L.S Zhai. Flow pattern and water holdup measurements of vertical upward oil-water two-phase flow in small diameter pipes. Int. J. Multiphase Flow., 41:91–105, 2012.

[48] H.W. Li, Y.L. Zhou, Y.D. Hou, B. Sun, and Y. Yang. Flow pattern map and time-frequency spectrum characteristics of nitrogen–water two-phase flow in small vertical upward noncircular channels. Exp. Therm. Fluid Sci., 54:47–60, 2014.

[49] L.S. Zhai, N.D. Jin, Y.B. Zong, Q.Y. Hao, and Z.K. Gao. Experimental flow pattern map, slippage and time-frequency representation of oil-water two-phase flow in horizontal small diameter pipes. Int. J. Multiphase Flow, 76:168–186, 2015.

[50] M.Y. Li, R.Q. Wang, J.B. Zhang, and Z.K. Gao. Characterizing gas-liquid two-phase flow behavior using complex network and deep learning. Chaos, 33:013108, 2023.

[51] M. Du, N.D. Jin, Z.K. Gao, and B. Sun. Analysis of total energy and time-frequency entropy of gas–liquid two-phase flow pattern. Chem. Eng. Sci., 82:144–158, 2012.

[52] S. Akcay, A. Atapour-Abarghouei, and T. P. Breckon. Ganomaly: Semi-supervised anomaly detection via adversarial training. In Computer Vision–ACCV 2018: 14th Asian Conference on Computer Vision, pages 622–637, 2019.

[53] Y.X. Liu, Y.F. Lin, Q.F. Xiao, G.H. Hu, and J. Wang. Self-adversarial variational autoencoder with spectral residual for time series anomaly detection. Neurocomputing, 458:349–363, 2021.

[54] X.W. Yu, X.N. Zhang, Y. Cao, and M. Xia. VAEGAN: A collaborative filtering framework based on adversarial variational autoencoders. In Proceedings of the 28th International Joint Conference on Artificial Intelligence, pages 4206–4212, 2019.

[55] Z. Bilicki and J. Kestin. Transition criteria for two-phase flow patterns in vertical upward flow. Int. J. Multiphase Flow, 13(3):283–294, 1987.

[56] W.J. Howarth. Coalescence of drops in a turbulent flow field. Chem. Eng. Sci., 19(1):33–38, 1964.

[57] M.J. Prince and H.W. Blanch. Bubble coalescence and break-up in air-sparged bubble columns. AIChE J., 36(10):1485–1499, 1990.

[58] A.E. Vardy and J. Brown. Transient turbulent friction in smooth pipe flows. J. Sound Vib., 259(5):1011–1036, 2003.